

# Surface plasmons on zig-zag gratings

Thomas J. Constant,<sup>1\*</sup> Tim S. Taphouse,<sup>2</sup> Helen J. Rance,<sup>1</sup> Stephen C. Kitson,<sup>2</sup> Alastair P. Hibbins,<sup>1</sup> and J. Roy Sambles<sup>1</sup>

<sup>1</sup>*Department of Physics and Astronomy, University of Exeter, Stocker Road, Exeter, Devon, EX4 4QL, UK*

<sup>2</sup>*Hewlett Packard Labs, Long Down Avenue, Stoke Gifford, Bristol, BS34 8QZ, UK*

\*[t.j.constant@ex.ac.uk](mailto:t.j.constant@ex.ac.uk)

**Abstract:** Optical excitation of surface plasmons polaritons (SPPs) on a 'zig-zag diffraction grating' is explored. The fabricated silver grating consists of sub-wavelength grooves 'zig-zagged' along their length, providing a diffractive periodicity to visible radiation. SPPs propagating in the diffraction plane and scattered by an odd number of grating vectors are only excited by TE polarized radiation, whereas for TM polarized light, which also induces surface charge, SPP excitation is forbidden by the grating's broken-mirror symmetry.

©2012 Optical Society of America

OCIS codes: (240.6680) Surface plasmons; (050.1950) Diffraction Gratings.

## References and links

1. R. W. Wood, "On a remarkable case of uneven distribution of light in a diffraction grating spectrum," *Proc. Phys. Soc. Lond.* **18**(1), 269–275 (1901).
2. S. J. Elston, G. P. Bryan-Brown, and J. R. Sambles, "Polarization conversion from diffraction gratings," *Phys. Rev. B Condens. Matter* **44**(12), 6393–6400 (1991).
3. W. L. Barnes, T. W. Preist, S. C. Kitson, J. R. Sambles, N. P. K. Cotter, and D. J. J. Nash, "Photonic gaps in the dispersion of surface plasmons on gratings," *Phys. Rev. B Condens. Matter* **51**(16), 11164–11167 (1995).
4. R. A. Watts and J. R. Sambles, "Reflection gratings as polarization converters," *Opt. Commun.* **140**(4-6), 179–183 (1997).
5. R. A. Watts, T. W. Preist, and J. R. Sambles, "Sharp surface-plasmon resonances on deep diffraction gratings," *Phys. Rev. Lett.* **79**(20), 3978–3981 (1997).
6. N. Bonod, G. Tayeb, D. Maystre, S. Enoch, and E. Popov, "Total absorption of light by lamellar metallic gratings," *Opt. Express* **16**(20), 15431–15438 (2008).
7. G. H. Welsh, N. T. Hunt, and K. Wynne, "Terahertz-pulse emission through laser excitation of surface plasmons in a metal grating," *Phys. Rev. Lett.* **98**(2), 026803 (2007).
8. B. K. Singh and A. C. Hillier, "Surface plasmon resonance imaging of biomolecular interactions on a grating-based sensor array," *Anal. Chem.* **78**(6), 2009–2018 (2006).
9. S. C. Kitson, W. L. Barnes, and J. R. Sambles, "Full photonic band gap for surface modes in the visible," *Phys. Rev. Lett.* **77**(13), 2670–2673 (1996).
10. R. A. Watts, J. B. Harris, A. P. Hibbins, T. W. Preist, and J. R. Sambles, "Optical excitation of surface plasmon polaritons on 90 and 60 bi-gratings," *J. Mod. Opt.* **43**, 1351–1360 (1996).
11. E. Popov, D. Maystre, R. C. McPhedran, M. Nevière, M. C. Hutley, and G. H. Derrick, "Total absorption of unpolarized light by crossed gratings," *Opt. Express* **16**(9), 6146–6155 (2008).
12. E. K. Popov, N. Bonod, and S. Enoch, "Comparison of plasmon surface waves on shallow and deep metallic 1D and 2D gratings," *Opt. Express* **15**(7), 4224–4237 (2007).
13. T. W. Ebbesen, H. J. Lezec, H. F. Ghaemi, T. Thio, and P. A. Wolff, "Extraordinary optical transmission through sub-wavelength hole arrays," *Nature* **391**(6668), 667–669 (1998).
14. K. Tetz, V. Lomakin, L. Pang, M. P. Nezhad, and Y. Fainman, "Polarization weighting of Fano-type transmission through bidimensional metallic gratings," *J. Opt. Soc. Am. A* **27**(4), 911–917 (2010).
15. Y. Chen, A. S. Schwanecke, V. Fedotov, V. V. Khardikov, P. L. Mladyonov, S. L. Prosvirnin, A. V. Rogacheva, N. I. Zheludev, and E. Huq, "Electron beam lithography for high density meta fish scale operational at optical frequency," *Microelectron. Eng.* **86**(4-6), 1081–1084 (2009).
16. B. H. Kleemann, J. Ruoff, and R. Arnold, "Area-coded effective medium structures, a new type of grating design," *Opt. Lett.* **30**(13), 1617–1619 (2005).
17. B. Bai, X. Meng, J. Laukkanen, T. Sfez, and L. Yu, "Asymmetrical excitation of surface plasmon polaritons on blazed gratings at normal incidence," *Phys. Rev. B* **80**, 1–11 (2009).
18. G. J. Kovacs, "Sulphide formation on evaporated Ag films," *Surf. Sci.* **78**(1), L245–L249 (1978).
19. S. Herminghaus, M. Klopfleisch, and H. J. Schmidt, "Attenuated total reflectance as a quantum interference phenomenon," *Opt. Lett.* **19**(4), 293–295 (1994).

20. D. J. Nash and J. R. Sambles, "Surface plasmon-polariton study of the optical dielectric function of silver," *J. Mod. Opt.* **43**, 81–91 (1996).
21. W. L. Barnes, T. W. Preist, S. C. Kitson, and J. R. Sambles, "Physical origin of photonic energy gaps in the propagation of surface plasmons on gratings," *Phys. Rev. B Condens. Matter* **54**(9), 6227–6244 (1996).
- 

## 1. Introduction

Surface plasmon polaritons (SPPs) are electromagnetic surface waves, bound to the interface between a dielectric and a conductor. Since the first recorded observation in 1902 [1], studies of the optical excitation of SPPs on metallic gratings have largely focused on single-pitch, parallel grooved mono-gratings [2–6]. SPPs on such gratings have been investigated recently as a method of terahertz frequency radiation generation [7], and as optical sensors for biomolecular interactions [8]. Other possible grating geometries, such as square or rectangular bi-gratings (comprised of two crossed mono-gratings) have also received attention [9–12]. Periodic arrays of holes in metal films, which are in essence simple bi-gratings, have also stimulated much interest over the last decade because of their enormously enhanced optical transmission [13,14] mediated by diffractively coupled SPPs. With the recent advances in large-area nano-fabrication, optical scientists are now able to explore more complex diffraction grating geometries [15–17]. Here, we study the optical excitation of diffractively coupled SPPs on a grating geometry with significantly reduced symmetry, a 'zig-zag' grating (Fig. 1).

## 2. Surface plasmon polaritons on zig-zag metal gratings

SPPs may be resonantly excited by an incident optical field that matches the mode's momentum, energy and field profile. The wavevector (in-plane momentum) of a SPP on a air/metal interface is larger than that available from a free-space photon, and so an in-plane momentum-enhancing mechanism is required to couple incident light to the SPP mode. One such mechanism is to pattern the metal periodically to form a diffraction grating, changing the in-plane wavevector of the surface fields by the addition or subtraction of an integer number of the grating wavevector ( $\mathbf{k}_{gx} = 2\pi \hat{x} / \lambda_{gx}$ ). The incident light must also be polarized so that it has a component of electric field normal to the grating surface, so that it may induce surface charges on the metal. For conventional gratings SPPs propagating in the plane of diffraction are excited only by TM polarized light.

In this letter, we use a zig-zag grating geometry as a SPP coupling mechanism to visible light. The zig-zag grating is formed of a surface-relief grating of sub-wavelength, and hence non-diffracting grooves which run along a silver surface. Perpendicular to this non-diffracting grating, the grooves are perturbed in the surface plane to introduce a long-pitch variation that may diffract visible light (Fig. 1). This 'zig-zag' perturbation introduces a diffracting pitch of  $\lambda_{gx}$ , which lies perpendicular to the short-pitch of the surface-relief grating,  $\lambda_{gy}$ . In many ways, the zig-zag geometry is similar to a conventional rectangular bi-grating, however, the long-pitch is present due to a zig-zag surface perturbation (not surface-relief grooves) and consequently the excitation of each diffractively coupled SPP is highly polarization selective. In addition the reduced symmetry of the zig-zag grating leads to two standing wave solutions at the first Brillouin Zone (BZ) which are degenerate in energy having no SPP band gap.

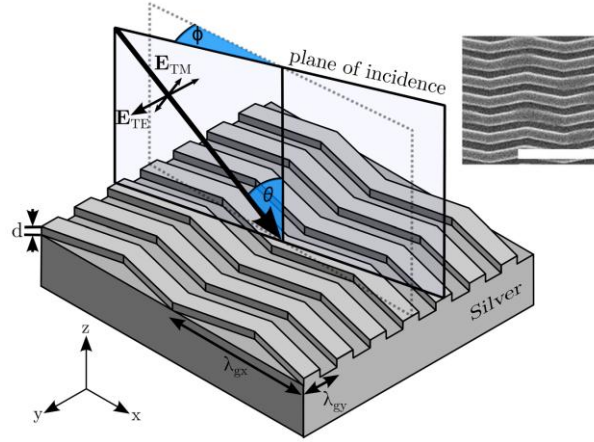


Fig. 1. The coordinate system of a zig-zag grating. The experimental sample parameters were  $\lambda_{gx} = 600$  nm,  $\lambda_{gy} = 150$  nm,  $d = 29.9$  nm with all measurements in this letter recorded at  $\phi = 0^\circ$ . Inset: A scanning electron micrograph of a replicated zig-zag surface in a polymer. (scale bar = 600 nm.)

The coordinate system used is outlined in Fig. 1. Plane polarized light illuminates the surface of the grating at a polar angle,  $\theta$ , and at an azimuthal angle,  $\phi$  (specifying the orientation of the grating vectors with respect to the plane of incidence). Zero azimuth ( $\phi = 0^\circ$ ) is when the plane of incidence contains the zig-zag grating vector,  $\mathbf{k}_{gx}$ . Notice that both Transverse Electric (TE) and Transverse Magnetic (TM) polarized light may provide an electric field component that lies normal to some part of the surface of the grating and hence induce surface charges, for all angles of incidence. Thus, given the necessary momentum matching conditions, either polarisation may excite SPPs. To provide further insight, a simple expression for the local normal component of electric field can easily be obtained by considering an approximation to the zig-zag surface given by,

$$\mathbf{r} = \mathbf{x} + \mathbf{y} + \cos(y - \cos(x))\hat{\mathbf{z}} \quad (1)$$

representing a zig-zag profile having unit amplitudes, and periodicities of  $2\pi$ . At normal incidence to the  $xy$  plane, the electric polarization vector of the electric field is defined as  $\mathbf{p} = \hat{\mathbf{x}}$  for TM and  $\mathbf{p} = \hat{\mathbf{y}}$  for TE polarizations. The normalized surface normal function and the magnitude of the polarization vector lying normal to the surface are then  $\hat{\mathbf{n}} = \partial_x \mathbf{r} \times \partial_y \mathbf{r} / |\partial_x \mathbf{r} \times \partial_y \mathbf{r}|$  and  $(\hat{\mathbf{n}} \cdot \mathbf{p})\hat{\mathbf{n}}$  respectively. The components,  $E_{TE}$  and  $E_{TM}$ , of the electric field normal to the surface, lying along the direction of propagation (the  $\hat{\mathbf{x}}$  direction) for both polarization cases, integrated over  $y$ , is then:

$$E_{TE} = \frac{4\pi \sin(x)}{\cos(2x) - 3} \quad (2)$$

$$E_{TM} = \frac{4\pi \sin^2(x)}{\cos(2x) - 3} \quad (3)$$

Both  $E_{TE}$  and  $E_{TM}$  are non-zero, so we may conclude that either polarization may induce surface charge and possibly excite SPPs. By expanding both these expressions as a Fourier sum in  $x$ , it is possible to find which in-plane wavevectors of incident light are required to match these field profiles. For incident light to match  $E_{TE}$  requires a series of only odd-ordered terms, while  $E_{TM}$  requires a series of only even-ordered terms. Diffracted fields at the surface will contain both odd and even wavevector components. Equations (2) and (3) predict

that TE polarized light will provide a suitable electric field distribution to enable the excitation of SPPs via only odd-ordered diffracted orders, while TM polarized light will excite SPPs only via even-ordered diffracted orders. This concept will be discussed again with reference to the experimental and modelled results in section 4.

### 3. Fabrication

A schematic of the experimental sample is shown in Fig. 1, comprising of a grating with a 600 nm zig-zag pitch ( $\lambda_{gx}$ ) to provide diffractive coupling to the SPPs. The periodicity of the non-diffracting surface-relief grooves ( $\lambda_{gy}$ ) is 150 nm.

A “master” of the zig-zag grating was produced in silicon using electron beam lithography. The pattern was exposed in PMMA using a write field of 400  $\mu\text{m}$  and a write field stitching error on the order of 20 nm. The exposed pattern was developed and reactive ion etched to a depth of  $70 \pm 10$  nm. This produced a 2.5  $\text{mm}^2$  grating on a silicon wafer. The structure was then duplicated in UV-cured polymer. Scanning electron microscopy was used to image the surface of this zig-zag grating, shown in Fig. 1. From this micrograph, the mark-to-space ratio of the grating structure was determined to be 0.25 with  $\lambda_{gx} = 600 \pm 5$  nm, and  $\lambda_{gy} = 150 \pm 5$  nm. This pattern was then transferred to another UV cured polymer (Norland Optical Adhesive 73 with an index of refraction  $n_{632.8\text{nm}} = 1.56$ ) and adhered to a glass substrate ( $n_{632.8\text{nm}} = 1.518$ ) using an embossing method.

Silver was thermally evaporated under high vacuum ( $5 \times 10^{-6}$  mbar) with 50 nm depositions followed by 10 minutes relaxation time repeated until an optically thick layer of 200 nm was recorded on the quartz crystal thickness monitor. This stepped procedure was used to prevent the temperature rising on the substrate enough to damage the polymer.

The substrate was then adhered to the back of a prepared glass hemisphere of radius 21.75 mm and refractive index  $n = 1.518$  using index matching fluid, the base of the hemisphere having been modified by removing 1 mm to account for the substrate thickness. This arrangement allows illumination of the embedded grating structure at the metal/glass interface at all angles of incidence. The mounting protects the surface of the silver from sulphur contamination [18], and preserves the fidelity of the grating profile, which would otherwise be shallowed at the air/metal interface by the addition of the silver. SPPs excited in these experiments propagate along the metal-glass interface.

### 4. Measurements and discussion

The reflected intensity of light from a zig-zag grating illuminated with TE polarized light, at a wavelength of 632.8 nm, was recorded as a function of the polar angle of incidence,  $\theta$  (Fig. 2). At  $\theta = 28^\circ$ , a minimum is observed in the TE reflectivity from the grating close to the first-order diffraction edge (calculated as  $37^\circ$ ), indicative of the excitation of a SPP that has been scattered by one grating vector,  $\mathbf{k}_{gx}$ . Incident light resonantly couples to this diffracted SPP and is scattered back in to the specular order with  $\pi$  phase retardation [19]. Out of phase with the specular reflection, a dark band is observed with the missing energy being dissipated as Joule heating. For comparison, the excitation of an in-plane SPP such as this on a mono-grating or bi-grating would require the light to be TM polarized. However, on this zig-zag grating for a SPP Bragg scattered by  $\mathbf{k}_{gx}$ , excitation with TM polarized light is forbidden (see section 2) and no minimum in the TM data is observed. The data agrees with theory from finite element method (FEM) modelling, also shown in Fig. 2, with fitting parameters of  $\epsilon_{632.8\text{nm}} = -17.5 + 0.55i$ , a groove depth of 29.9 nm, and a mark-to-space ratio of 0.25. Surface roughness and small groove profile changes from the embossing method are not accounted for in the modelling.

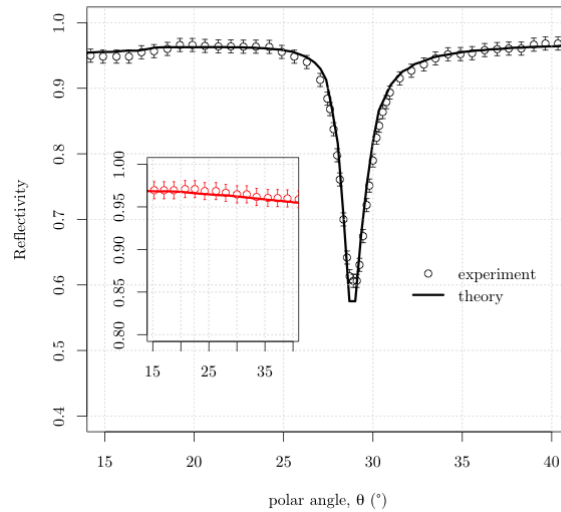


Fig. 2. Specular reflectivity of TE (black) and TM (red) polarized light as a function of polar angle,  $\theta$ , with a wavelength of 632.8 nm,  $\phi = 0^\circ$ . Circles: recorded data with error bars of 1%, line: fitted numerical model prediction.

The dispersion of the SPPs is mapped as a function of in plane wavevector,  $\mathbf{k}_x$ , by varying the polar angle  $\theta$ , an angular frequency,  $\omega$ , using a polarized, collimated, monochromatic beam, produced by a white light source together with a spectrometer, in the wavelength range  $400 < \lambda_0 < 850$  nm (Intensity of reflected light is monitored with a photomultiplier).

The reflectivity of incident TE polarized light at  $\phi = 0^\circ$  is shown in Fig. 3. Bands of low reflectivity are a result of a resonant excitation of SPPs mapping thereby the dispersion curves of the SPPs. Two Bragg-scattered SPP dispersion curves are observed for this polarization case, one originating at  $-\mathbf{k}_{gx}$  and one originating at  $+3\mathbf{k}_{gx}$ . These odd-order diffracted SPs are excited by TE polarized light. The SP dispersion curve from a  $+2\mathbf{k}_{gx}$  scattering is missing as, on a zig-zag grating, it is not excited by TE polarized light as predicted by Eq. (2). Using the fitted parameters from Fig. 2, the dispersion plots were reproduced from FEM modelling and found to be in good agreement and are shown in Fig. 3. The small difference between the model asymptotic limits of the SPs and experiment may be attributed to the differences between the dielectric function of silver used for the model [20] and our experimental sample. One anticipates that  $2\mathbf{k}_{gx}$  diffracted SPPs may be excited by TM polarized light, however the zig-zag surface profile presented does not contain any  $2\mathbf{k}_{gx}$  components. Thus for SPPs to gain  $2\mathbf{k}_{gx}$  in wavevector they will require two scatterings by  $\mathbf{k}_{gx}$  a process which, while not forbidden, is inherently weak. To facilitate strong coupling by even-order scattered SPPs and TM polarized light, an even  $\mathbf{k}_{gx}$  component has to be added to the zig-zag profile, but this removes the mirror symmetry of the grating and the polarization selectivity would be destroyed.

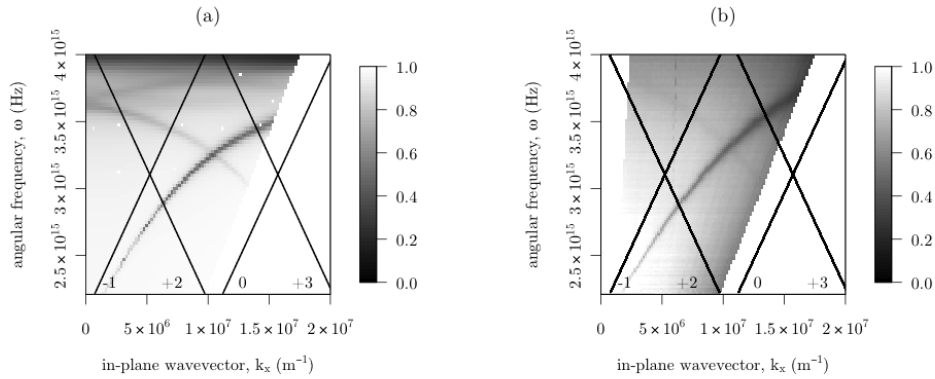


Fig. 3. TE polarized reflectivity as a function of in-plane wavevector and angular frequency, mapping the SPP dispersion on a zig-zag grating. (a) Numerical prediction and (b) measured data. Solid lines show the positions of diffracted light lights scattered by  $m\mathbf{k}_{gx}$ , where  $m = -1, +2, 0, +3$ .

Normally at Brillouin zone (BZ) boundaries, diffractive coupling results in two counter propagating SPPs, which establish a standing wave [21]. The two standing wave solutions correspond to different field distributions with respect to the grating profile, and between these two energy solutions no surface modes propagate: a SPP band gap forms. However, the dispersion relation shown in Fig. 3 and the predictions from FEM modelling shows no measurable SPP band gaps at the first BZ boundaries for this zig-zag grating. Generally, the in-plane wavevector of a standing SPP wave is half that of the total Bragg vector by which the two counter propagating SPPs have been scattered. For the  $-\mathbf{k}_{gx}$  and  $+\mathbf{k}_{gx}$  scattered SPPs, crossing at the first BZ, the SPP wavevector is  $3\mathbf{k}_{gx}/2$ . Through symmetry, there are two possible solutions for this standing wave on a zig-zag grating, with the areas of high field of one solution shifted spatially by  $\lambda_{gx}/4$  with respect to the other solution. Because of the zig-zag reflection symmetry, the arrangements of these two field solutions on the zig-zag surface are equivalent. The solutions are degenerate in energy and therefore no band gaps at the first BZ are observed.

## 5. Conclusions

We have demonstrated experimentally and with FEM modeling the coupling of plane polarized light to SPPs on a metallic zig-zag grating. We have found that when the plane of incidence contains the zig-zag grating vector, odd-order diffracted SPPs couple only to TE polarized light and coupling to TM light is forbidden. At the first BZ boundary in this orientation, photonic band-gaps do not form because the two possible standing wave solutions along the zig-zag surface are equivalent in energy. Changing the zig-zag symmetry will allow control of the polarization selectivity of SPP coupling on such gratings, with asymmetric zig-zag gratings providing a route to polarization independent excitation of SPPs which propagate in the plane of diffraction

## Acknowledgments

The authors are grateful for technical support from Mr. N Cole and for the financial support of EPSRC through grant EP/G022550/1 and HP Labs Bristol.